Islamic Azad University

Journal of
Optoelectronical Nanostructures

Winter 2020 / Vol. 5, No. 1

Effect of Variation of Specifications of Quantum Well and Contact Length on Performance of Inp-Based Vertical Cavity Surface Emitting Laser (VCSEL)

Abbas Ghadimi*,[1], Mohammad Ahmadzadeh[2]

[1] Department of Electrical Engineering, Lahijan Branch, Islamic Azad University, Lahijan, Iran

[2] Department of Electrical Engineering, Rasht Branch, Islamic Azad University, Rasht, Iran

(Received 12 Dec. 2019; Revised 21 Jan. 2020; Accepted 20 Feb. 2020; Published 15 Mar. 2020)

Abstract: In this study, the effects of variation of thickness and the number of quantum wells as well as the contact length were investigated. In this paper, a vertical cavity surface emitting laser was simulated using of software based on finite element method. The number of quantum wells was changed from 3 to 9 and the results which are related to output power, resonance wavelength and threshold current were extracted. Output specifications in terms of quantum wells thicknesses of 3.5nm to 9.5nm were evaluated. Contact thickness is also changed from 0.5µm to 3µm. Results showed that as the number of quantum wells increased, the resonance wavelength also increased and photon energy decreased. By reducing the thickness of the quantum well, the threshold current and radiation wavelength were also decreased. By increasing the contact length, threshold current and output power increased. Temperature inside the network and density of photon were increased as the contact length increased.

Keywords: Quantum Well, Contact Length, Threshold Current, Output Power, Vertical Cavity Surface Emitting Laser (VCSEL)

1. INTRODUCTION

Invention the first Laser in 1960, opened new gates to discover various types of these devices. Semiconductor lasers provided a wide field for researchers and gained particular importance among the various types of semiconductor lasers [1-3]. Vertical Cavity Surface Emitting Laser (VCSEL) comparing with Edge Emitting Laser has owned more applications. Edge emitting semiconductor lasers had many disadvantages such as: difficult testing process, the need for more current in order to produce same output and low speed and low efficiency. All these disadvantages have caused that almost all researches in the field of

* Corresponding author. Email: **ghadimi@liau.ac.ir**

semiconductor lasers are about VCSEL.

A VCSEL is consist of an active region which is located between two distributed Brag reflectors (DBR). The thickness of each layer above and below the reflector is equal to one quarter of radiation wavelength. Several quantum

wells are located in the center of device and two separator layers are located in two sides symmetrically. Two separator layers create a confinement to trap the effective carriers and optical confinement. The thickness of active region is only in nanometer range. In this small active region of VCSELs and due to reduction of losses, the DBRs should have more reflectivity. Series resistance in the upper reflector is the most important problem in VCSELs. A suitable way for decreasing of series resistance is changing of doping. The change of doping increases output power and reduces the recombination as well as threshold current and effects on the efficiency [4].

In [5], the effects of doping concentration are investigated, but the effects of thickness variations and the number of quantum wells were not investigated. The structure which is presented in this paper, has lower threshold current and higher gain than which has been introduced in [6]. The effect of changing of doping concentration of DBR layer in the GaN-VCSEL was studied. In the report [7], the improved lasing performance of the III-nitride based vertical-cavity surface-emitting laser (VCSEL) was demonstrated. The threshold current density was reduced in the device. Design, simulation and analysis of VCSEL at different wavelengths were presented in [8]. In [9], an AlGaAs/GaAs-based VCSEL in the wavelength of 850nm was simulated. Threshold current of 1mA, with a maximum slope efficiency of 0.66W/A were obtained. In [10], the nonlinear rate equations governing a quantum dot laser was used to simulate the transient behavior of the laser. In [11], the frequency behavior of the tunnel junction quantum dot VCSEL was investigated by using an analytical numerical method. A new laser structure was theoretically investigated using simulation software PICS3D.Lower threshold current and higher output power were obtained in [12]. In [13] generating and controlling of the rogue waves were investigated.

In this paper, a VCSEL is simulated and effect of variation of thickness and number of quantum wells and effect of change of contact length on the output parameters such as threshold current, output power and density of photon are investigated. The diagram of network temperature variation, power and threshold current versus the changing of contact length is investigated. Fig. 1 shows the structure of laser with wavelength length of 1550nm. In this structure, six $In_{0.76}Ga_{0.24}\ As_{0.82}P_{0.18}$ quantum wells with thickness of 5.5nm and $In_{0.48}Ga_{0.52}\ As_{0.82}P_{0.18}$ barriers with thickness of 8nm of as active regions are used.

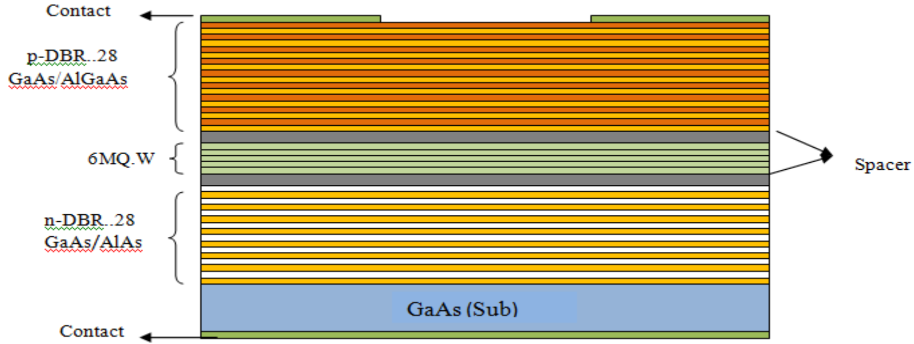

Fig. 1 Schematic structure of VCSEL

We served rate equation as an efficient description of the basic lasing behavior of VCSEL [10].

$$\frac{dP}{dt} = GP + R_{sp} - \frac{P}{\tau_p} \tag{1}$$

$$\frac{dN}{dt} = \frac{I}{q} - \frac{N}{\tau_c} - GP \tag{2}$$

Where P, N, R_{sp}, τ_p, τ_c are number of photons, number of electrons and photon life time, electron life time, respectively. Gain, threshold current and optical power calculated from below equations [10].

$$G = \frac{\Gamma V_g \sigma_g}{v}\left(N - N_0\right) \tag{3}$$

$$I_{th} = \frac{q}{\tau_c}\left(N_0 + \frac{1}{\tau_p G_N}\right) \tag{4}$$

$$P = \frac{\tau_p}{q}\left(I - I_{th}\right) \tag{5}$$

Γ, V_g, N_0 are quantum confinement factor, group velocity and transparency density, respectively.

Energy of photon is obtained from Eq. 6:

$$E(ev) = \hbar.\omega = \frac{\hbar \times 2\pi \times c}{\lambda} \tag{6}$$

Where c is light speed, λ is wavelength and h is Plank constant.
For $In_wGa_{1-w}AS_yP_{1-y}$, the band gap energy is obtained from Eq. 7 [14]:

$$E_g = 1.34w(1-y) + 0.354wv + 2.78(1-w)(1-v) + 1.432(1-w)y \tag{7}$$

By solving recursive equation, the values of 0.76 and 0.82 are obtained for w and y, respectively. The Band gap energy for barrier material is also higher. For $In_{0.76}Ga_{0.24}As_{0.82}P_{0.18}$ as quantum well material, band gap energy is calculated and equal to 1.05eV.

Quantum wells are located between two InP separator layers which is separated from GaAs reflectors layer. Thickness of cavity is 0.735µm which is nearly half of length of radiation wave (1.55µm). Upper DBR layers are composed of 28 pair of $Al_{0.67}Ga_{0.33}$ As /GaAs layer in periodic mode. In lower DBR there are 28 pair of layers composed of GaAs/AlAs. Refractive index of AIAs, GaAs and $Al_{0.67}Ga_{0.33}As$ are 2.89, 3.38 and 3.05, respectively. Thickness of each layer is calculated from Eq. 4 [15].

$$H = \lambda \frac{\lambda}{4 \times n} \tag{8}$$

Where, n is reflective index, λ is radiative wavelength and H is thickness of layer. GaAs substrate is used in the device which has the thickness equal to half of wavelength. Table. 1 shows the device and material parameters.

Table.1: Device and material parameters

Layer	Material	Thickness(µm)	Refractive Index	Doping(/cm3)
Substrate	GaAs	0.707	3.38	**10^{18} (donor)**
Top mirror	$GaAs/Al_{0.67}Ga_{0.33}As$	0.114/0.127	3.38/2.05	**$10^{18}/10^{18}$ (acceptor)**
Bottom mirror	GaAs/AlAs	0.114/0.127	3.38/2.89	**$4*10^{17}/4*10^{17}$ (donor)**
Quantum well	$In_{0.76}Ga_{0.24}As_{0.82}P_{0.18}$	0.006	3.5	**-------**
Barrier	$In_{0.76}Ga_{0.24}As_{0.82}P_{0.18}$	0.008	3.5	**-------**
Top spacer	GaAs/InP	0.045 /0.278	3.38/3.15	**$4*10^{19}/10^{18}$ (acceptor)**
Bottom spacer	GaAs/InP	0.045 / 0.278	3.38 / 3.15	**$5*10^{17}/10^{18}$(donor)**
Top Contact	GaAs	0.304	3.38	**$4*10^{17}$ (acceptor)**
Bottom Contact	GaAs	0.020	3.38	**$5*10^{18}$ (donor)**

2. SIMULATION AND RESULTS

2.1: Investigation of the effect of number of quantum well on the output specifications

The number of quantum well is changed from 3 to 9. The most important issue that is seen in the present section is the variation of resonance wavelength of the device, which increases with increasing the number of quantum wells. Obviously, the maximum photon energy in the device is for a case with 3 quantum wells. Fig. 2 shows the variation of wavelength and energy with the number of quantum wells.

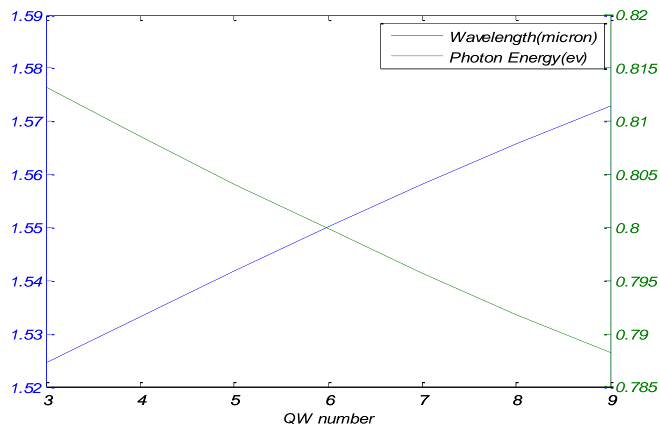

Fig. 2 wavelength and photon energy versus the number of quantum wells.

When number of quantum wells increases, threshold current also increases. In two case with 3 and 4 quantum wells, the threshold current is very low and for more than 5 quantum wells the threshold current increases. Fig.3 shows the variation of threshold current based on the number of quantum wells.

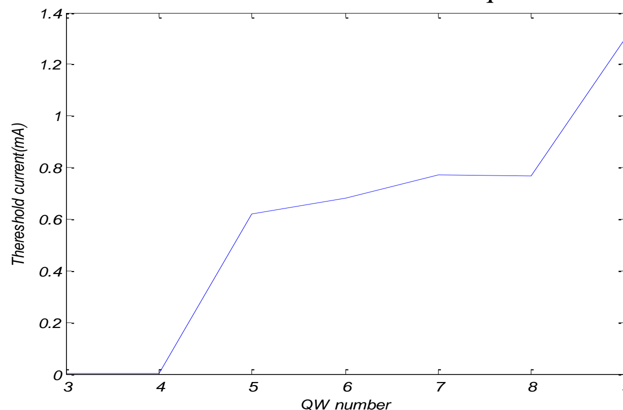

Fig. 3 Threshold current versus the number of quantum wells.

When the number of quantum wells decreases, the active region becomes smaller, the volume of active region and the threshold current are both decrease. When the diameter of the device is equal to one wavelength, no more than 3 quantum wells in the active area can be considered. Because the thickness of the barrier may be less than the thickness of the well, there will be tunneling between the wells and consequently no radiation recombination will occur in the wells [16-18]. But if we take the cavity length as a factor of four wavelengths (in this structure), we cannot produce more than three quantum wells. The voltage-current curve shows that; it is possible to calculate the series resistance of DBR layers in specific voltages. Table. 2 shows the measured values with changing the number of quantum wells in the device. It can be seen that the 6 quantum wells are the best choice for the device.

Table. 2 Output parameters with changing the number of quantum wells.

Number of Wells	Threshold Current(ma)	Temperature Inside the Grid	Radiation Wavelength	E(ev)	Output Power(mw)	Gain
3	Very low	305.4	1.52	0.813	Very low	28.9
4	Very low	305.5	1.53	0.808	Very low	37.7
5	0.62	307.1	1.54	0.804	27.12	24.4
6	0.685	307.3	1.55	0.8	28.42	31.4
7	0.773	307.1	1.56	0.795	26.06	18.54
8	0.77	307.3	1.56	0.791	27.78	30.4
9	1.3	307.2	1.57	0.788	27.5	37.1

Output power is another important parameter among the output specifications of the device. Fig. 4 shows the variation of output power versus voltage.

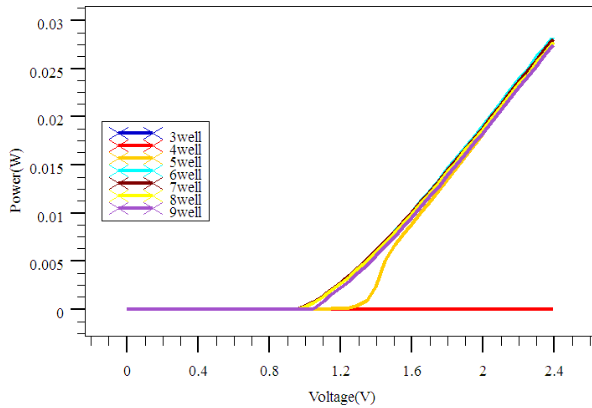

Fig. 4 Output power versus voltage for different the number of quantum wells.

In voltage of 2.4v, the output power is very low for cases with 3 and 4 quantum wells; it can be seen that the maximum of output power is occurred for 6 quantum wells and bias of 2.4v. The minimum and maximum gain in the active region are observed for 7 and 4 quantum wells, respectively (Fig. 5).

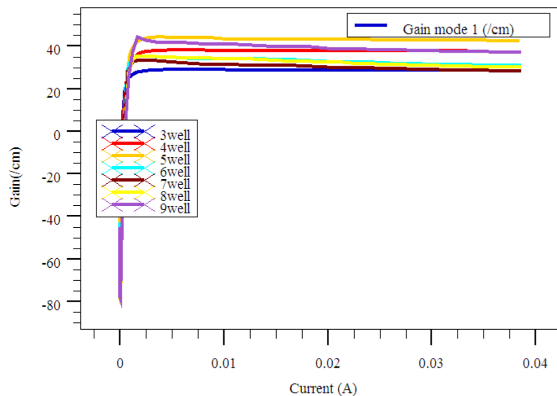

Fig. 5 Gain versus current for different number of quantum wells.

One of the important results that can be seen from the curve of power versus voltage is for the case the device with 3 and 4 quantum wells that is shown in Fig. 6.

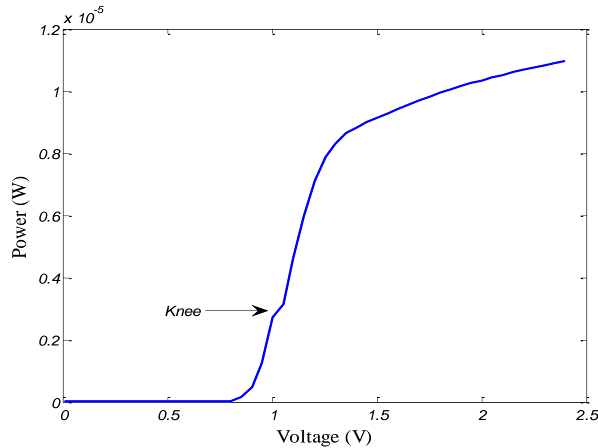

Fig. 6 A knee in diagram of power versus voltage in device with 4 quantum wells.

It can be seen that in bias of about 1v, there is a knee in diagram. This knee is related to spontaneous emission. This shows that before stimulated emission, injected current has more participation in spontaneous emission. For the case with 3 and 4 quantum wells there is carrier leakage from active layers.

Output power of the device versus number of quantum wells is shown in Fig.7.

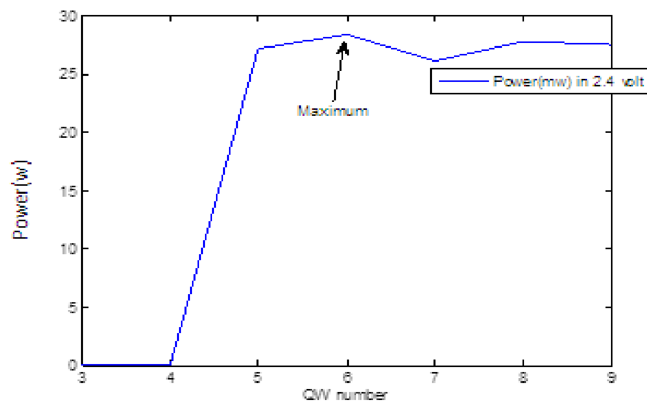

Fig. 7 Power versus number of quantum wells

There is a point that when the diameter of the device is equal to wavelength, it is not possible to consider more than 3 quantum wells, because the thickness of barrier may be lower than the thickness of well and tunneling may not occurred between wells and as a result, the radiative recombination in well is not occurred. Because of the structure design with specified values, radiative recombination in QWN of 6 to 7 is less for QWN of 5 to 6.

2.2: The effect of change of quantum well thickness on the output specifications

The other parameter that its effect on the performance of VCSEL have been investigated is thickness of quantum well. Table.3 shows the variation of output specifications of the device with change of thickness of quantum well.

Table. 3: Output specifications of device with change of thickness of quantum well.

Thickness (nm)	Threshold Current(ma)	Output Power(mw)	Gain	Wavelength(nm)	Photon Energy	Temperature Inside the Grid
3.5	0.603	27.51	32.69	1542	0.803	307.2
4.5	0.65	27.45	30.89	1546	0.801	307.2
5.5	0.689	27.37	28.25	1551	0.79	307.2
6.5	0.703	27.33	26.1	1553	0.797	307.2
7.5	0.722	27.22	24.64	1557	0.796	307.2
8.5	0.731	26.89	23.26	1561	0.794	307.2
9.5	0.748	26.52	22.03	1564	0.792	307.2

The thicknesses of wells are selected 3.5nm to 9.5nm, respectively. The thickness of cavity is sum of thickness of active regions and spacer layers. The cavity thickness, temperature and barrier thickness is 75nm, 300K and 8nm, respectively. The minimum and maximum threshold current are for the cases with quantum well thickness of 3.5nm and 7.5nm, respectively.

Output power is calculated at voltage of 2.4v and Fig. 8 shows the variation of threshold current and output power versus quantum well thickness. In thickness of 5.5 nm, as can be seen from Table. 3, radiation wavelength is 1551 nm which has the lowest shift relative to defined wavelength (1550 nm).

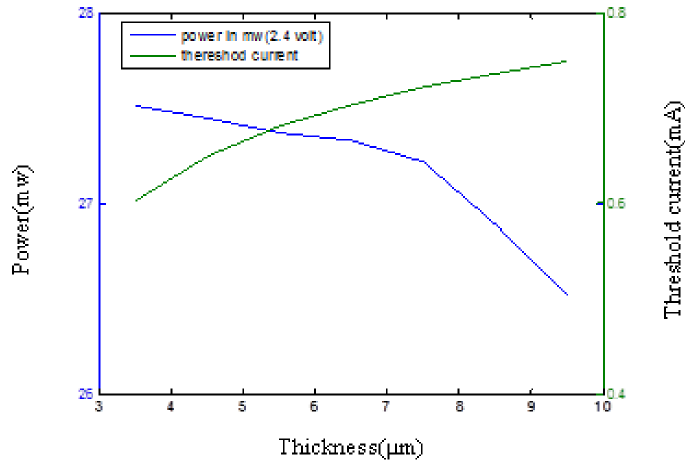

Fig. 8 Variation of threshold current and output power for various thicknesses of quantum wells.

The variation of wavelength and photon energy with variation of well thickness is shown in Fig. 9.

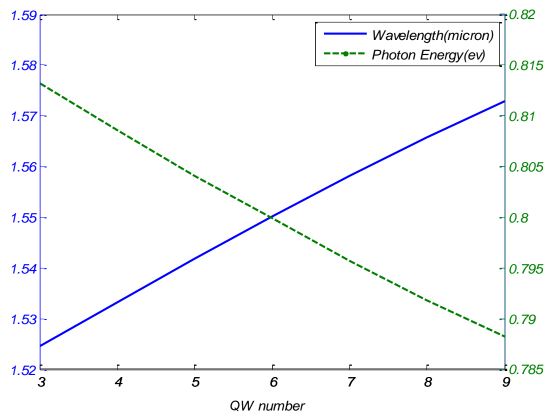

Fig. 9 Variation of wavelength and photon energy versus variation of thickness of quantum well.

Due to the overlapping of resonance spectrum of cavity in the gain region, by increasing the thickness of quantum well, the threshold gain reduced.

Fig. 10 shows the variation of threshold gain in terms of well thickness.

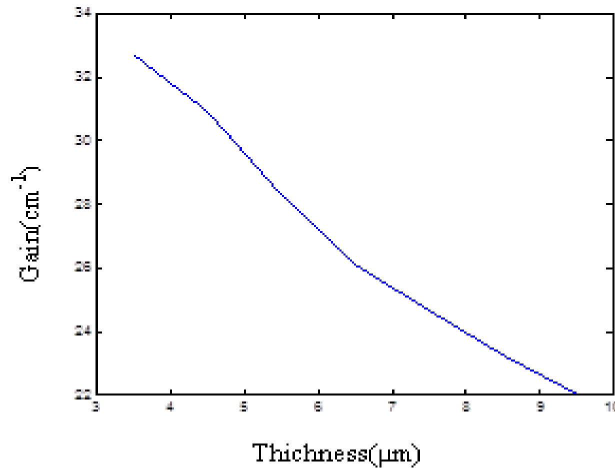

Fig. 10 Threshold gain versus quantum well thickness.

2.3: The effect of contact length on the output specifications

Table. 4 shows the variations of output specification of VCSEL lasers versus the variation of contact length.

Table. 4 Output specifications of device by changing the contact length.

Contact Length	Threshold Current(ma)	Power(mw)	Photon Density	Gain	Temperature Inside the Grid
0.5	0.668	6.57	$1.89*10^5$	33.8	304
1	0.677	7.21	$2.11*10^5$	33.07	305.8
1.5	0.681	7.62	$2.23*10^5$	32	306.7
2	0.685	8.01	$2.29*10^5$	31.26	307.3
3	0.687	8.13	$2.32*10^5$	31.13	307.9

Fig.11 shows the diagram of photon density with changing of contact length at voltage of 1.5v. It is obvious that if the contact surface is increased, the density of the photons will increase.

The threshold current and output power increased by increasing the contact length, which is shown in Fig. 12.

Temperature in the device is increased by increasing the contact length as well as by increasing the threshold current. Fig. 13 shows the diagram of temperature with increase in contact length.

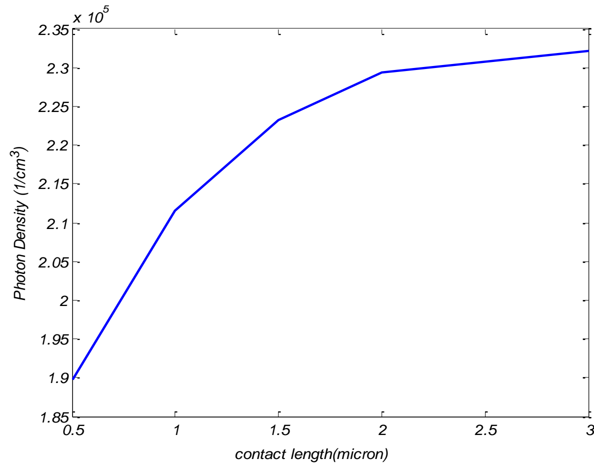

Fig. 11 photon density variation versus contact length.

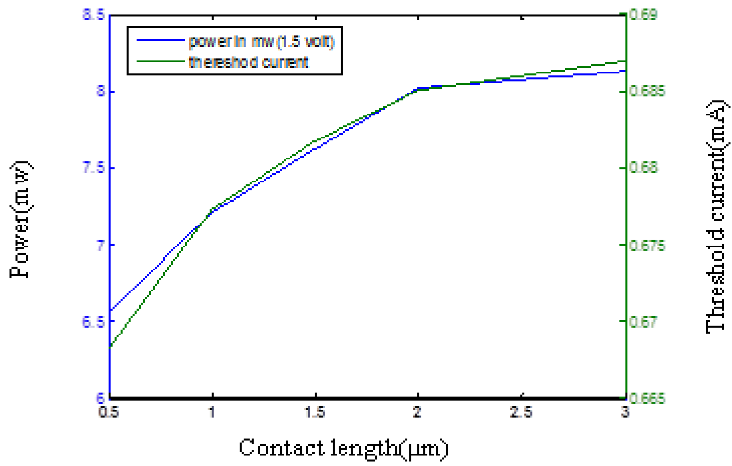

Fig. 12: Power and threshold current versus contact length.

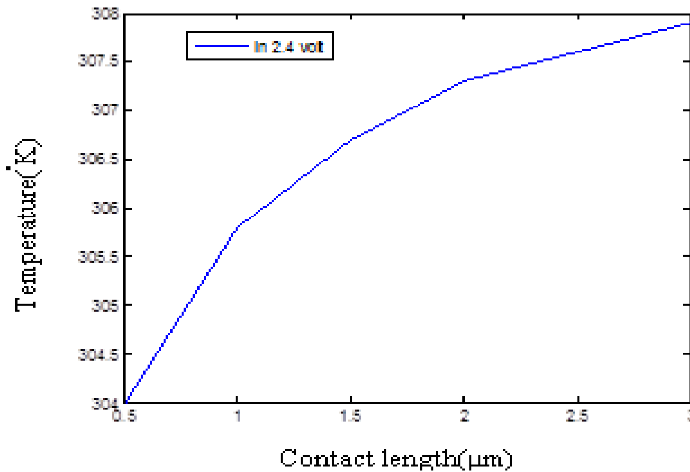

Fig. 13: Device temperature versus the contact length.

3. CONCLUSION

In this article, the effects of changing of thickness and the number of quantum wells as well as contact length on the performance of VCSEL were investigated. A simulation of VCSEL was performed with MATLAB and Silvaco software. The VCSEL has 6 quantum wells which has two distributed Brag reflectors at top and bottom. Device used a GaAs substrate with the thickness of half of the wavelength. The radiative wavelength is 1.55μm. The number of quantum wells was changed from 3 to 9, and the output specifications were studied. The results showed that with increasing of the number of quantum wells, resonance wavelength increased and photon energy decreased. For 3 and 4 quantum wells, the value of threshold current is very low and after that by increasing the number of quantum wells, the threshold current also increased. In the case with 6 quantum wells the maximum output power is obtained from the device and for 7 quantum wells, the minimum gain was observed.

The thickness of quantum well was changed and the output specifications were observed. By reducing the thickness of quantum wells, the threshold current and the radiation wavelength were reduced. In the device 5.5nm quantum wells, the minimum wavelength shifts from the wavelength of 1.5μm was observed.

Also, the contact width was changed from 0.5μm to 3μm and the output specifications are observed and tabulated. By increasing the contact length, the threshold current and output power were increased. Temperature inside the device was also increased. By increasing the contact length, photon density was increased.

REFERENCES:

[1] K. Murali Krishna, M. Ganesh Madhan, *Numerical Simulation of High-Temperature VCSEL Operation and Its Impact on Digital Optical Link Performance*, Presented at Nano Elec. Circuits and Com. Sys., (2018, August), [Online]. Available: https://link.springer.com/chapter/10.1007/978-981-13-0776-8_31.

[2] Vladimir P. Kalosha, Vitaly A. Shchukin, Nikolay Ledentsov, Nikolay N. Ledentsov, Comprehensive *Analysis of Electric Properties of Oxide-Confined Vertical-Cavity Surface-Emitting Lasers*, IEEE Journal of Sel. Top. in Quantum Elec., [Online]. 25(6) (2019, July),1-9 ,Available: https://ieeexplore.ieee.org/abstract/ document/ 8765 756.

[3] A. I. Nashed, Michel Lestrade, Z. Q. Li, Z. M. Simon Li, *Efficient Optical Modeling of VCSELs using Full-Vectorial FDFD method,* Presented at International Conference on Numerical Simulation of Optoelectronic Devices (NUSOD), (2019, July) [Online]. Available: https://ieeexplore.ieee.org/abstract/document/8806850.

[4] R Sarzala, W Nakwaski, *Methods to improve performance of the 1.3µm Oxide Confined GaInNAs/GaAs quantum well VCSELs*, 12th International Conference on Transparent Optical Networks(ICTON), (2010, June) [Online]. Available: https://ieeexplore.ieee.org/document/5549020.

[5] R Sarzala, L Piskorsi, R Kurdawiec, W Nakwaski, *Optimization of GaInNAs quantum well VCSEL emitting at 2.33 µm,* App. Phys. A, [Online]. 115(3), (2014, June) 961-969, Available: https://link.springer.com/article/10.1007/s00339-013-7915-9.

[6] P.S Menon, K Kandiah, S Sharri, N.Y Majlis, *Comparison of mesa and device diameter variation in double wafer- fused multi quantum-well, long wavelength, VCSELs*, Sains Malaysiana, [Online]. 6(40), (2011, November) , 631-636, Available: https://www.semanticscholar.org/paper/InP-based-multi-quantum-well-mole-fraction-effects-Visvanathan-Shaari/58b2febc711943d3ba9a3aea11ef7a7f34fab215.

[7] D. H. Hsieh, A. J. Tzou, T. S. Kao, F. I. Lai, D. W. Lin, B. C. Lin, T. C. Lu, W. C. Lai, C. H. Chen, and H. C. Kuo, *Improved carrier injection in GaN-based VCSEL via AlGaN/GaN multiple quantum barrier electron blocking layer*, Optic. Exp., [Online]. 23(21), (2015,Oct) 27145-27151, Available: https://www.osapublishing.org/oe/ abstract.cfm?uri=oe-23-21-27145.

[8] Priyanka Goyal; Mohit Sharma; Ananya Jha; Monika Kumari; Somendra P. Singh; Nikita Singh, Gurjit Kaur, *Design and analysis of VCSEL LASER for*

third window of optical communication system, 2016 International Conference on Electrical, Electronics, and Optimization Techniques (ICEEOT), [Online]. Available: https://ieeexplore.ieee.org/document/7755512.

[9] Huize Fan; Kai Liu; Qi Wei; Min Zhang; Xiaomin Ren; Yongqing Huang; Xiaofeng Duan, *The simulation of monolithic vertical integration of VCSEL and RCE photodiode,* 16th International Conference on Optical Communications and Networks (ICOCN), (2017, Aug), [Online]. Available: https://ieeexplore.ieee.org/ document/8121413.

[10] P.V. Mena; J.J. Morikuni; S.-M. Kang; A.V. Harton; K.W. WyattA, *simple rate-equation-based thermal VCSEL model,* J. Light wave. Tech., [Online]. 17(5), (1999, May), 865 – 872, Available: https://ieeexplore.ieee.org/document/762905.

[10] M.Rezvani. J, *Simulation of Direct Pumping of Quantum Dots in a Quantum Dot Laser*," JOPN. [Online]. 2(2), (2017), 61-70, Available: http://jopn.miau.ac.ir/ article_2425.html.

[11] M. Riahinasab, E.Darabi*, Analytical Investigation of Frequency Behavior in Tunnel Injection Quantum Dot VCSEL*, ," JOPN. [Online]. 3(2), (2018), 65-86, Available: http://jopn.miau.ac.ir/article_2876.html.

[12] Z. Danesh. K, *Improving Blue InGaN Laser Diodes Performance with Waveguide Structure Engineering*," JOPN. [Online]. 4(1), (2019), 1-26, Available: http://jopn.miau.ac.ir/article_3382.html.

[13] M.Zaki, M.hosseini, *Controlling the Occurrence of Rogue Waves in an Optically Injected Semiconductor Laser via Changing The Injection Strength*,"JOPN. [Online]. 2(3), (2017), 39-46, Available: http://jopn.miau.ac.ir/article_2430.html.

[14] Farah Z, Jasim, Khalid Omar and Z.Hassan, *Multiple quantum well of GaAs VCSEL structure*, Journal of Opt. and adv. Mat., [Online]. 11(11), (2009, November), 1723-1727, Available: https://old.joam.inoe.ro/ index.php?option= magazine&op =view &idu=2222&catid=44.

[15] A.Ghadimi, M.Ahmadzadeh, *The Effect of Doping Change in Distributed Bragg Reflector (DBR) Layers on the Operation at Different Temperatures of an InP-based Vertical Cavity Surface Emitting Laser (VCSEL)*," Lasers. In. Eng. [Online]. 40 (2018) 149–159, Available:https://www.oldcitypublishing.com/journals/lie-home/lie-issue-contents/lie-volume-40-number-1-3-2018/lie-40-1-3-p-149-159/.

[16] Zandi Goharrizi, Gh. Alahyarizadeh, Z.Hassan, H.Abu Hassan, *Low-dimensional Systems and Nanostructures,"* Physica E. [Online]. 50 (2013, May) 61-66, Available: https://www.sciencedirect.com/science/article/pii/S1386947713000532.

[17] Yuta Suzuki, Shin-ichiro Tezuka, *Numerical simulation of 3D Fox–Li integral equation described by Rayleigh–Sommerfeld diffraction for MEMS-VCSEL,"* Optical Review [Online]. 26 (2019, October) 430-435, Available: https://link.springer.com/article/10.1007/s10043-019-00551-1

[18] Karan Mehta, Yuh-Shiuan Liu, Jialin Wang, Hoon Jeong, Theeradetch Detchprohm, P. Douglas Yoder, Russell D. Dupu, *Thermal Design Considerations for III-N Vertical-Cavity Surface-Emitting Lasers Using Electro-Opto-Thermal Numerical Simulations,"* IEEE Journal of Quantum Electronics [Online]. 55(5) (2019, October) 1-8. Available: https://ieeexplore.ieee.org/abstract/document/8817911